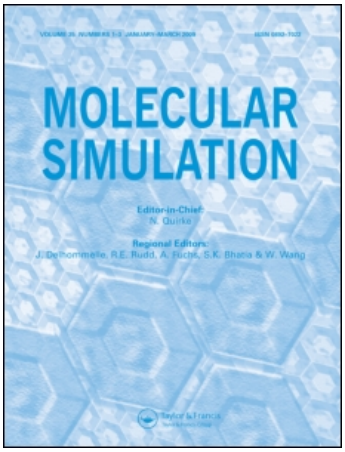

Molecular Simulation
Publication details, including instructions for authors and subscription information:
http://www.informaworld.com/smpp/title~content=t713644482

How does the Electrostatic Force Cut-Off Generate Non-uniform Temperature Distributions in Proteins?

Koji Oda[a]; Hiroh Miyagawa[a]; Kunihiro Kitamura[a]
[a] Research Center, Taisho Pharmaceutical Co., Ltd., No. 403, Saitama, Japan

To cite this Article Oda, Koji , Miyagawa, Hiroh and Kitamura, Kunihiro(1996) 'How does the Electrostatic Force Cut-Off Generate Non-uniform Temperature Distributions in Proteins?', Molecular Simulation, 16: 1, 167 — 177
To link to this Article: DOI: 10.1080/08927029608024070
URL: http://dx.doi.org/10.1080/08927029608024070

Molecular Simulation, 1996, Vol. 16, pp. 167–177
Reprints available directly from the publisher
Photocopying permitted by license only

HOW DOES THE ELECTROSTATIC FORCE CUT-OFF GENERATE NON-UNIFORM TEMPERATURE DISTRIBUTIONS IN PROTEINS?

KOJI ODA, HIROH MIYAGAWA and KUNIHIRO KITAMURA

Research Center, Taisho Pharmaceutical Co., Ltd., No.403, Yoshino-cho 1-chome, Ohmiya-shi, Saitama.330, Japan

(Received March 1995, accepted July 1995)

Molecular dynamics simulations (MDS) with electrostatic force cut-off on heterogeneous molecular systems make temperature separation between solute and solvent [1–4]. In MDS where the temperature separation occurs, we found that there is a non-uniform temperature distribution in protein. The pattern of temperature distribution was shown to be peculiar to the protein, suggesting a possible relationship between dynamical and thermal properties of protein. By principal component analysis, the non-uniform temperature distribution was ascribed to high temperature of large fluctuation modes in protein. Further analysis by thermal diffusion equation between principal modes showed that in protein large fluctuation modes inherently have smaller value of heat capacity than small fluctuation modes have and are easily heated up by truncation noise due to abrupt cut-off of electrostatic forces.

KEY WORDS: Molecular dynamics, cut-off approximation of electrostatic force, temperature control, principal component analysis, heat capacity.

1 INTRODUCTION

Recently, molecular dynamics simulation (MDS) is widely used to elucidate structural behavior of biomolecules, leading to design new proteins and drugs [5]. Since MDS requires large amount of computational time, the cut-off of electrostatic long-range force has been employed as a conventional tool to reduce the computational time. In these days, however, some questions are posed for the use of the cut-off from the following aspects; affects on energy conservation [2, 4, 6], on atomic fluctuation [3, 6–8] and on dielectric properties [7, 9], disagreements with X-ray structures and with MDS results without the cut-off [3, 4, 6–8, 10] and occurrence of temperature separation between solute and solvent in heterogeneous molecular system [1–4]. These discrepancies are caused by truncation noise due to abrupt cut-off of electrostatic forces, which comes from going-in and/or going-out of the atoms near-by the surface of cut-off sphere, as well as, the neglect of long range contribution of electrostatic forces.

Here, we shall concentrate on temperature separation in protein, which nobody has reported to date. The temperature separation between solute and solvent is commonly observed in the MDS in the case that electrostatic forces are abruptly truncated and temperature control is applied to prevent increase of system

temperature with truncation noise, and as a result solvent is always hotter than solute [1–4]. This temperature separation problem is not completely solved at present [2]. We found that temperature separation is also generated in protein in such a manner that respective amino acid residues keep different temperature given from the system, which does not change with time and with their initial temperature, resulting in the non-uniform temperature distribution peculiar to the protein. Even though the non-uniformity of temperature comes from cut-off artifacts, the peculiar pattern of non-uniform temperature distribution in the protein gave us a chance to elucidate an inherent relationship between dynamical and thermal properties of protein. Thus, we applied principal component analysis on protein fluctuation [11–13] and ascribed the non-uniform temperature distribution to high temperature of large fluctuation modes in protein. The considerations on thermal diffusion between principal modes showed that the non-uniformity of temperature between principal modes comes from the stronger truncation noise on large fluctuation modes than on small fluctuation modes. Furthermore, the non-uniformity is emphasized by inherently smaller value of heat capacity of large fluctuation modes in protein. The precise derivation is described below.

2 METHOD

2.1 *Preparation of the Molecular System*

The protein structure used here is that of *Ras* p21 with GTP, which was built up based on X-ray structure of *Ras* p21-GTP (guanosine triphosphate) analogue complex [14]. For MDS, AMBER4 program [15] was used. Then, energy parameters, AMBER/OPLS [16] and TIP3P [17] were used for *Ras* p21 complex and water molecule, respectively. For Lennard-Jones parameter of Mg^{2+}, Åqvist's value [18] was employed. Partial atomic charges in GTP were assigned using Merz-Kollman method [19,20] based on the result of molecular orbital calculation with STO-3G basis set by Gaussian 92 [21]. SHAKE [22] constraints were applied to hydrogen atoms, time step was 2fs, and temperature control was of Berendsen [23] with coupling time of 0.2 ps.

Hydrogen atoms were added to the X-ray structure and the whole structure was minimized for 100 steps with the heavy atoms constrained at their initial X-ray coordinates in order to remove van der Waals contacts of added hydrogen atoms. Then, the protein was placed at the center of a 32 Å radius sphere which consists of water molecules and again the whole structure was minimized for 100 steps with the protein atoms constrained. 2 ps run with tight coupling (scaling velocity of each atom at every step) to 10 K heat bath and the following 2 ps run in 100 K were performed. After that, the system was coupled to 300 K heat bath.

2.2 *Conditions of Electrostatic Force Cut-off*

MD runs were done under the following conditions of electrostatic force cut-off: (a) Abrupt cut-off at 8 Å (abbreviate as C8), (b) Abrupt cut-off at 12 Å (C12), (c) No

cut-off (NC) and (d) Cut-off by switching (or smoothing) function [1,2,4,6,7,24] (SW). Practically, in C8 and C12, electrostatic forces were calculated according to the atom 'pair-list' made by residue based cut-off to avoid splitting the residue dipoles [15]; when any atom of a residue is in the cut-off sphere, all atoms of the residue are included to the atom pair-list. The atom pair-list was made at every 50fs in the runs. In SW, the cut-off was done with the electrostatic potential multiplied by $S(r)$ which has the following form:

$$\begin{aligned} S(r) &= 1 && \text{for } r \leqslant r_L, \\ S(r) &= 1 - 10\left(\frac{r-r_L}{r_U-r_L}\right)^3 + 15\left(\frac{r-r_L}{r_U-r_L}\right)^4 - 6\left(\frac{r-r_L}{r_U-r_L}\right)^5 && \text{for } r_L < r \leqslant r_U, \\ S(r) &= 0 && \text{for } r > r_U. \end{aligned} \tag{1}$$

The second form of $S(r)$ is a fifth-order polynomial that smoothly connects $S(r)=1$ to $S(r)=0$, avoiding the truncation noise. Here, $S(r)$ was used with $r_L = 8.0$ Å and $r_U = 12.0$ Å.

For computation, CRAY-EL92 and Kubota TITAN2-800 were used in C8 and C12. In NC, SUN SPARCstation 2 with a hardware accelerator for non-bonded force calculations, MD-Engine (MDE), was used, which was developed by K. Kitamura and his group [25,26]. MDE used in this study consists of 6 processor boards and the computation speed is about 2GFLOPS. MDE was also used in SW since any one-variable function for non-bonded force calculation can be applied in MDE.

3 RESULTS AND DISCUSSION

3.1 Non-uniform Temperature Distribution

Figure 1 shows that temperature separation between solute and solvent appears under C8 and C12 as reported elsewhere [1−4], but not in NC and SW. It is also observed that temperature of the whole system is raised up from the reference temperature (300 K) in C8 and C12 while the temperature is kept well to the reference temperature in NC and SW, suggesting that the truncation noise due to abrupt cut-off works to raise the system temperature against the temperature control. Because the temperature separation between solute and solvent is observed in C8 and C12 but not in SW, the separation is not due to the neglect of long range contribution of electrostatic forces but due to the truncation noise.

Figure 1 also shows that the temperature separation between solute and solvent in C8 and C12 does not disappear during simulation time. In fact, the same extent of temperature separation remained even when C8 was continued till 116 ps (data not shown). Furthermore, the temperature separation is also observed in simulations with different initial conditions. Figure 2 depicts that the temperature profiles of 8 Å and 12 Å force cut-off simulations (abbreviated as NC–C8 and NC–C12 respectively) started with a 36 ps configuration in NC where the temperature separation is

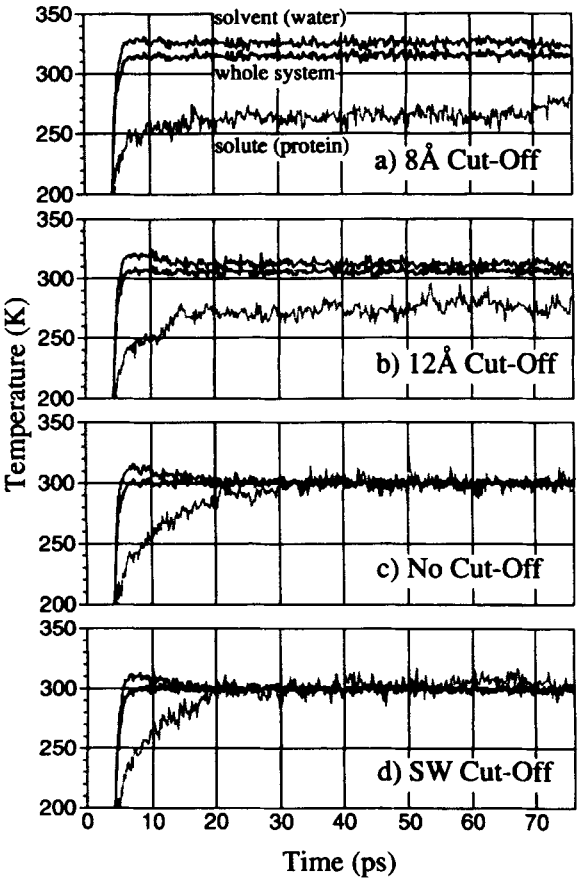

Figure 1 Temperature profiles during the simulations. Temperature separation between solute (protein) and solvent (water) is observed in C8 (a) and C12 (b) but not in NC (c) and SW (d). Explanations for abbreviations C8, C12, NC and SW, see text.

not observed. Again, the same extent of temperature separation as that in Figure 1 appeared. Thus, the temperature separation does not change with time and with initial condition.

In C8 and C12, it is surprising that temperature is different among amino acid residues in protein as shown in Figure 3, while it is nearly equal to the reference temperature in NC and SW. Hence, the non-uniform distribution of residue temperature is also caused by the truncation noise as well as the temperature separation between solute and solvent. Water molecules around the protein also have non-uniform temperature distribution affected by the nearby amino residues in C8 and C12 (data not shown).

The non-uniformity of temperature in protein does not change with time in an abrupt cut-off simulation. Figure 4 shows correlation diagrams of residue temperature averaged over 20 ps in the different simulation time ranges. In the abrupt cut-off simulation, temperature of some particular residues is steadily high and that of the

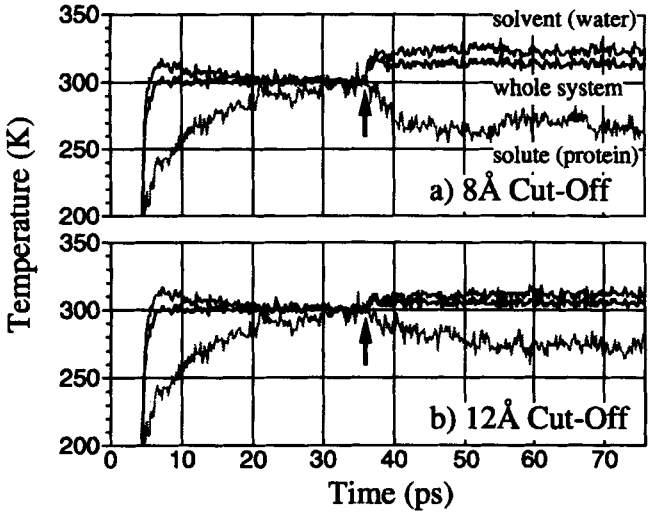

Figure 2 Temperature profiles of 8 Å and 12 Å cut-off simulations. NC–C8 (a) and NC–C12 (b) were started with a 36ps configuration in NC (indicated by arrow). The temperature separation between solute (protein) and solvent (water) is observed again with the same extent as in Figure 1.

other particular residues is steadily low and the pattern of non-uniform temperature distribution is unchanged. On the other hand, there is not such definite pattern in the no cut-off simulation. Furthermore, the pattern of temperature distribution does not change by initial condition. As in Figure 5, the patterns are also similar to each other between C8 and NC–C8 and between C12 and NC–C12. Consequently, the pattern of temperature distribution in the abrupt cut-off simulation is intrinsic for respective protein because the pattern does not change with time and with initial condition.

3.2 Generation Mechanism of the Non-Uniform Temperature Distribution

As mentioned above, though the non-uniform temperature distribution in protein is induced by the truncation noise due to the abrupt cut-off of electrostatic forces, the pattern of residue temperature distribution has a peculiar form to the respective protein. This prompts us to elucidate a relationship between dynamical and thermal properties of protein. For this purpose, generation mechanism of the non-uniform temperature distribution was investigated by means of principal component analysis.

Principal component analysis is a powerful tool to describe dynamics of protein [11–13], where internal fluctuation of protein is expressed by principal axes (*i.e.*, modes) that are eigen vectors of variance-covariance matrix of atomic displacements in protein. A principal axis represents the orientation and the relative magnitude of cooperative fluctuation of atoms and the corresponding eigen value shows the square amplitude of the fluctuation. In this study, the analysis is applied on the fluctuations of α-carbon (C_α) atoms of the protein. Temperature of a principal mode

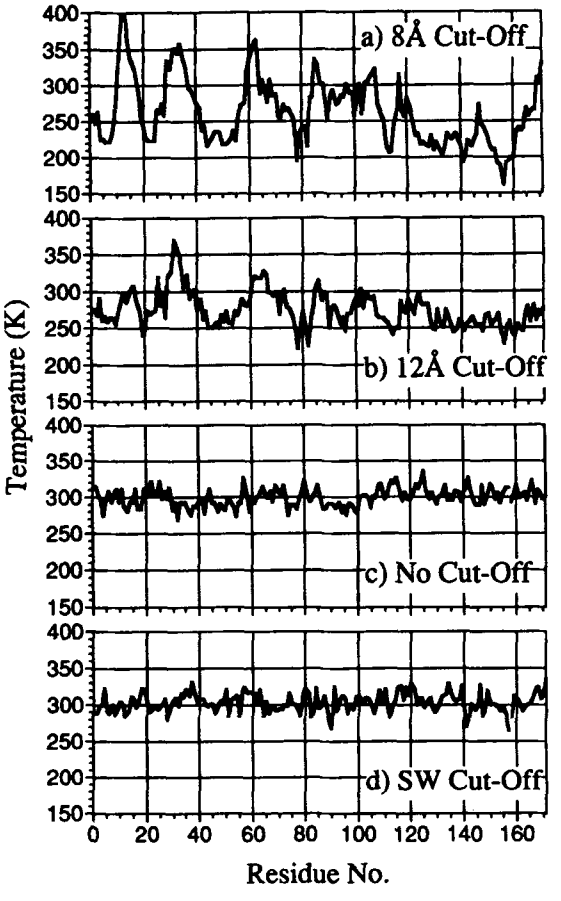

Figure 3 Temperature distributions in the protein. Residue temperature was averaged over 40 ps ($t = 36 \sim 76$ ps). Non-uniform temperature distributions are observed in C8 (a) and C12 (b). On the other hand, uniform temperature distributions are observed in NC (c) and SW (d).

is defined by projection of velocity of C_α atoms onto the principal axes as follows.

$$T_i = \frac{2}{k_B} \sum_{l:\text{atom}} \frac{1}{2} m_l (\dot{\mathbf{x}}_l \cdot \mathbf{q}_i^l)^2, \tag{2}$$

where k_B is Boltzmann constant and m_l and $\dot{\mathbf{x}}_l$ are mass and velocity of atom l. $\mathbf{q}_i$ is the normalized vector representing i-th principal axis and $\mathbf{q}_i^l$ is its component of atom l. T_i is the instantaneous temperature of the mode i. Figure 6 shows averaged temperature of principal modes, where the principal modes are arranged in descending order of their amplitude. In C8, the large fluctuation modes have higher temperature than the small ones. Thus, the non-uniform temperature distribution in protein is ascribed to high temperature of large fluctuation modes in protein.

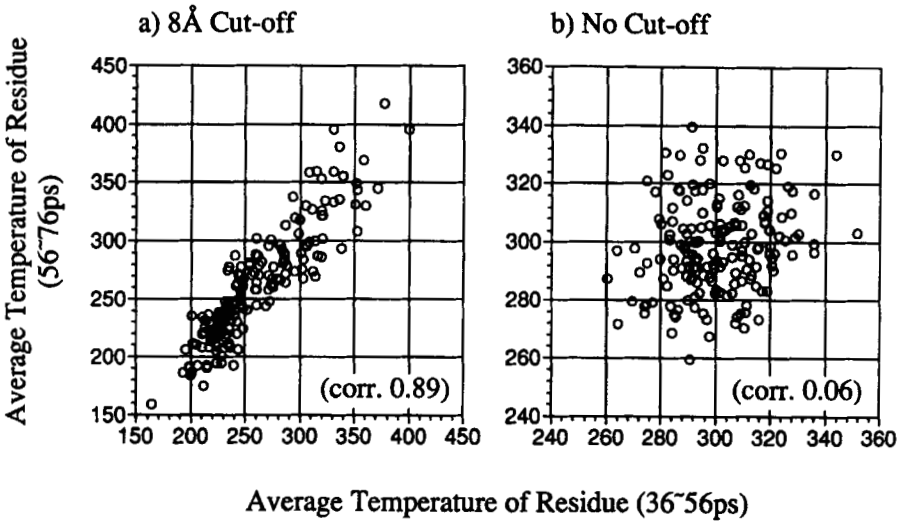

Figure 4 Correlation diagrams of residue temperature averaged over 20 ps in the different time ranges, 36 ~ 56 ps (x axis) and 56 ~ 76 ps (y axis). In case (a), the correlation coefficient shows 0.89 between two temperature distributions of different time ranges, but 0.06 in case (b).

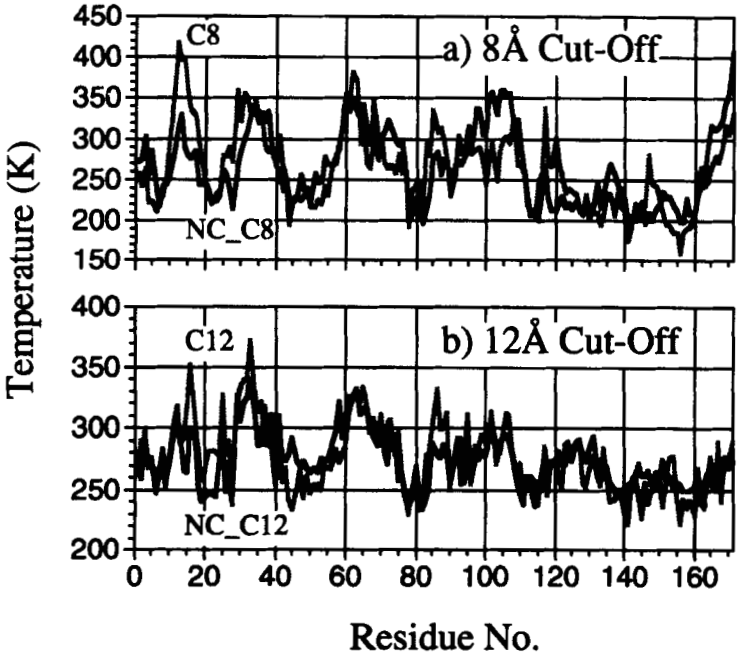

Figure 5 Temperature distributions in simulations with different initial conditions. Shaded line is of C8 and C12 (see Figure 1) and solid line is of NC–C8 and NC–C12 (see Figure 2). The residue temperature is averaged over 20 ps ($t = 56 \sim 76$ ps). The patterns of temperature distribution in protein are similar to each other despite the difference in initial condition.

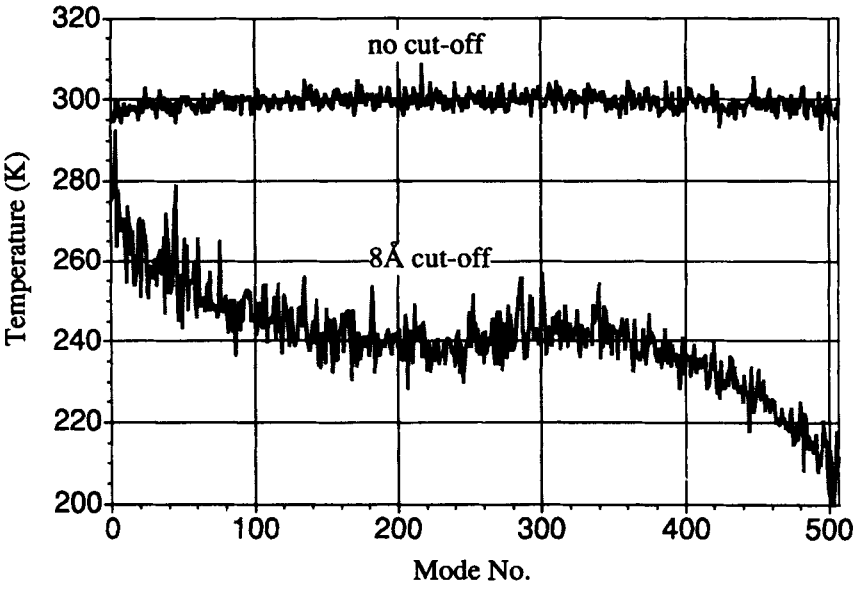

Figure 6 Temperature of each principal mode averaged over 40 ps ($t = 56 \sim 96$ ps). Principal modes were arranged in descending order of amplitude of fluctuation. In C8, large fluctuation modes have higher temperature than small ones while all the modes have same temperature in NC.

To explain this temperature difference between modes, thermal diffusion equation between principal modes is useful.

$$\frac{\partial E_i}{\partial t} = -\sum_{j \neq i} L_{ij}(T_i - T_j) + (P_i + B_i), \tag{3}$$

where E_i represents total energy of mode i, L_{ij} is microscopic thermal conductivity between mode i and j, and P_i is energy given by truncation noise. B_i is energy given by Berendsen's temperature control and is expressed as

$$B_i = \frac{1}{\tau}\left(\frac{T_0}{T} - 1\right) \cdot T_i, \tag{4}$$

where T_0 is temperature of the heat bath, T the instantaneous temperature of the whole system and τ the coupling constant to the heat bath. Then, rewriting equation (3) by $\partial T_i/\partial t = \partial T_i/\partial E_i \cdot \partial E_i/\partial t = 1/C_i \cdot \partial E_i/\partial t$ where C_i is heat capacity of mode i defined as $C_i \equiv (\partial E_i/\partial T_i)$, we obtain

$$\frac{\partial T_i(t)}{\partial t} = -\sum_{j \neq i} \lambda_{ij} C_j (T_i - T_j) + \frac{1}{C_i}(P_i + B_i). \tag{5}$$

Here, the relation $L_{ij} = \lambda_{ij} C_i C_j$ is used because L_{ij} is proportional to C_i and the equality $L_{ij} = L_{ji}$ should be satisfied as the Onsager reciprocity relation. In steady

state, the averaged temperature of mode i is written as

$$\langle T_i \rangle_t = \frac{\sum_{j \neq i} \lambda_{ij} C_j \langle T_j \rangle_t}{\sum_{j \neq i} \lambda_{ij} C_j} + \frac{1}{C_i} \cdot \frac{\langle P_i \rangle_t + \langle B_i \rangle_t}{\sum_{j \neq i} \lambda_{ij} C_j}, \tag{6}$$

where $\langle \rangle_t$ represents time averaging. The second term comes from the simulation artifacts, that is, the truncation noise due to abrupt cut-off and the Berendsen's temperature control. Without those artifacts, temperature of each mode is represented by the first term, geometric average of temperature of the other modes weighted by $\lambda_{ij} C_j$; temperature of the mode i is determined by temperature of the other modes through the microscopic conductivity between modes.

At equilibrated state in NC and SW, because truncation noise does not exist and the system temperature is kept to the reference temperature T_0 (see Figure 1), $\langle P_i \rangle_t = \langle B_i \rangle_t = 0$. Thus, the solution of equation (6) is given by $\langle T_i \rangle_t = \langle T_j \rangle_t$ for any i and j. Therefore, all the modes have same temperature as in Figure 6.

In C8 and C12, because truncation noise exists and the system temperature is shifted up from the reference temperature T_0, $\langle P_i \rangle_t > 0$ and $\langle B_i \rangle_t < 0$. Practically, large $\langle P_i \rangle_t$ and $\langle B_i \rangle_t$ values compared with the heat coupling term $\Sigma_{j \neq i} \lambda_{ij} C_j$ make non-uniform temperature distribution and determines its pattern as follows. $|\langle B_i \rangle_t|$ is large for high $\langle T_i \rangle_t$ and small for low $\langle T_i \rangle_t$ because of equation (4). Then, the subtraction term $\langle B_i \rangle_t$ contributes to flattening of the distribution. Hence $\langle B_i \rangle_t$ is not the leading term of the non-uniform temperature distribution. On the other hand, $\langle P_i \rangle_t$ becomes large corresponding to the amplitude of fluctuation mode, making temperature of large fluctuation modes high. This is because large fluctuation of an atom makes exchanges of the interacting atoms nearby the surface of cut-off sphere more frequent, producing the stronger effect of truncation noise on the atom. As equation (6) shows, $\langle P_i \rangle_t$ raises $\langle T_i \rangle_t$ through the heat capacity C_i. In general, heat capacity is related to temperature fluctuation. Thus, the heat capacity of mode i is estimated from temperature fluctuation of the corresponding mode using the following equation,

$$C_i = \frac{k_B \langle T_i \rangle_t^2}{\langle (T_i - \langle T_i \rangle_t)^2 \rangle_t}. \tag{7}$$

As shown in Figure 7(a), large fluctuation modes give large relative temperature fluctuation. This tendency is also observed in no cut-off condition (see Figure 7(b)). So large temperature fluctuation of large fluctuation modes is not due to a cut-off artifact but to an intrinsic property of the protein, that is, large fluctuation modes inherently have smaller value of heat capacity. Consequently, both $\langle P_i \rangle_t$ and C_i in equation (6) serve that large fluctuation modes have high temperature.

By principal component analysis, we have shown that the large fluctuation modes in protein have smaller value of heat capacity than small modes have. In contrast, all the modes have the same heat capacity $1/2\, k_B$ when protein motion is described in normal mode, *i.e.*, a set of harmonic oscillators. So the heat capacity difference between principal modes is considered as an appearance of anharmonicity in large

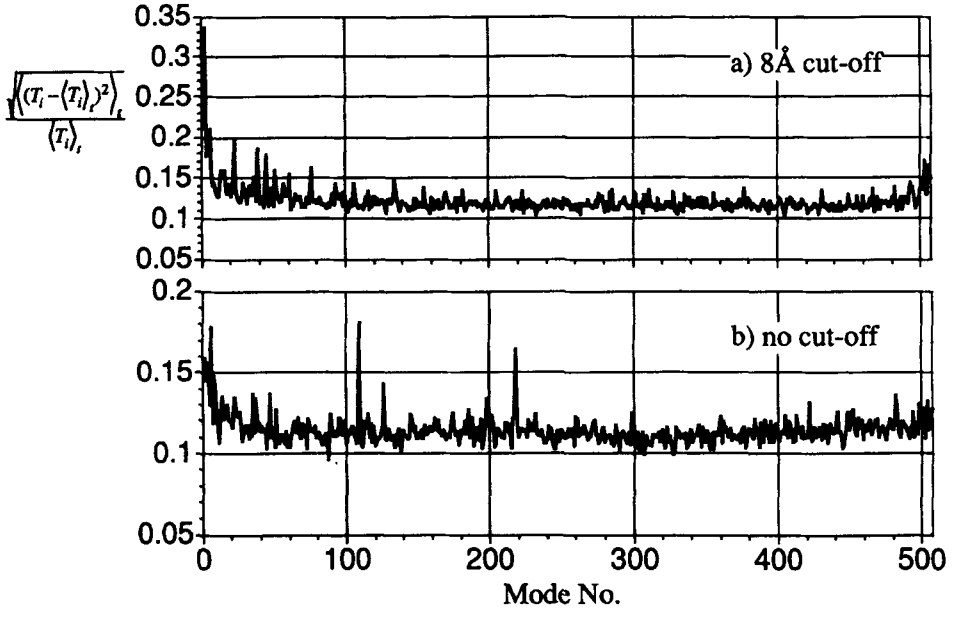

Figure 7 Relative temperature fluctuation of principal modes. Large fluctuation mode has large relative temperature fluctuation both in C8 (a) and in NC (b).

principal modes, corresponding to the previous report [11–13] that large fluctuation modes are cooperative anharmonic motions, while small fluctuation modes are harmonic motions of protein.

4 CONCLUSION

The truncation noise due to abrupt cut-off of electrostatic forces strongly influences temperatures of large fluctuation modes in protein because the large fluctuation modes inherently have smaller value of heat capacity, generating the non-uniform temperature distribution in protein. This also explains why the temperature separation occurs between solute and solvent: relative temperature fluctuation of water atoms is observed to be much larger than that of protein atoms, meaning smaller value of heat capacity of water atoms. Hence, solvent is always hotter than solute.

Acknowledgements

We would like to thank Dr. A. Kitao, Mr. S. Sunada and Dr. F. Hirata for helpful advice and discussion. This study was supported in part by Special Coordination Funds from the Science and Technology Agency of the Japanese Government.

References

[1] M. Levitt and R. Sharon, "Accurate simulation of protein dynamics in solution", *Proc. Natl. Acad. Sci.*, **85**, 7557 (1988).

[2] D. B. Kitchen, F. Hirata, J. D. Westbrook, R. Levy, D. Kofke and M. Yarmush, "Conserving Energy during Molecular Dynamics Simulations of Water, Proteins, and Proteins in Water", *J. Comp. Chem.*, **11**, 1169 (1990).

[3] J. Guenot and P. A. Kollman, "Molecular dynamics studies of a DNA-binding protein: 2. An evaluation of implicit and explicit solvent models for the molecular dynamics simulation of the *Escherichia coli trp* repressor". *Protein Science*, **1**, 1185 (1992).

[4] J. Guenot and P. A. Kollman, "Conformational and Energetic Effects of Truncating Nonbonded Interactions in an Aqueous Protein Dynamics Simulation", *J. Comp. Chem.*, **14**, 295 (1993).

[5] W. F. van Gunsteren, P. K. Weiner and A. J. Wilkinson, eds, ESCOM, Leiden, *Computer Simulation of Biomolecular Systems Vol. 2* (1993).

[6] R. J. Loncharich and B. R. Brooks, "The Effects of Truncating Long-Range Forces on Protein Dynamics", *PROTEINS*, **6**, 32 (1989).

[7] P. E. Smith and B. M. Pettitt, "Peptides in ionic solutions: A comparison of the Ewald and switching function techniques", *J. Chem. Phys.*, **95**, 8430 (1991).

[8] M. Saito, "Molecular dynamics simulations of proteins in solution: Artifacts caused by the cutoff approximation", *J. Chem. Phys.*, **101**, 4055 (1994).

[9] H. Schreiber and O. Steinhauser, "Molecular dynamics studies of solvated polypeptides: why the cut-off scheme does not work", *Chem. Phys.*, **168**, 75 (1992).

[10] H. Schreiber and O. Steinhauser, "Cutoff Size Does Strongly Influence Molecular Dynamics Results on Solvated Polypeptides", *Biochemistry*, **31**, 5856 (1992).

[11] A. Kitao, F. Hirata and N. Gō, "The Effects of Solvent on the Conformational and the Collective Motions of Protein: Normal Mode Analysis and Molecular Dynamics Simulations of Melittin in Water and in Vacuum", *Chem. Phys.*, **158**, 447 (1991).

[12] S. Hayward, A. Kitao, F. Hirata and N. Gō, "Effect of Solvent on Collective Motions in Globular Protein", *J. Mol. Biol.*, **234**, 1207 (1993).

[13] A. Amadei, A. B. M. Linssen and H. J. C. Berendsen, "Essential Dynamics of Proteins", *PROTEINS*, **17**, 412 (1993).

[14] M. V. Milburn, L. Tong, A. M. deVos, A. Brünger, Z. Yamaizumi, S. Nishimura and S. -H. Kim, "Molecular Switch for Signal Transduction: Structural Differences Between Active and Inactive Forms of Protooncogenic *ras* Proteins", *Science*, **247**, 939 (1990).

[15] D. A. Pealman, D. A. Case, J. C. Caldwell, G. L. Seidel, U. C. Singh, P. Weiner and P. A. Kollman, AMBER 4.0 University of California (1991).

[16] W. L. Jorgensen and J. Tirado-Rives, "The OPLS Potential Functions for Proteins. Energy Minimizations for Crystals of Cyclic Peptides and Crambin.", *J. Am. Chem. Soc.*, **110**, 1657 (1988).

[17] W. L. Jorgensen, "Transferable Intermolecular Potential Functions for Water, Alcohols, and Ethers. Application to Liquid Water", *J. Am. Chem. Soc.*, **103**, 335 (1981).

[18] J. Åqvist, "Ion-Water Interaction Potentials Derived from Free-Energy Perturbation Simulations", *J. Phys. Chem.*, **94**, 8021 (1990).

[19] U. C. Singh and P. A. Kollman, "An Approach to Computing Electrostatic Charges for Molecules", *J. Comp. Chem.*, **5**, 129 (1984).

[20] B. H. Besler, K. M. Merz, Jr. and P. A. Kollman, "Atomic Charges Derived from Semiempirical Methods", *J. Comp Chem.*, **11**, 431 (1990).

[21] M. J. Frisch G. W. Trucks, M. Head-Gordon, P. M. W. Gill, M. W. Wong, J. B. Foresman, B. G. Johnson, H. B. Schlegel, M. A. Robb, E. S. Replogle, R. Gomperts, J. L. Andres, K. Raghavachari, J. S. Binkley, C. Gonzalez, R. L. Martin, D. J. Fox, D. J. Defrees, J. Baker, J. J. P. Stewart and J. A. Pople, Gaussian 92 Revision G.1, Gaussian, Inc. (1992).

[22] J. P. Ryckaert, G. Ciccotti and H. J. C. Berendsen, "Numerical integration of the cartesian equations of motion of a system with constraints: Molecular dynamics of n-alkanes", *J. Comp. Phys.*, **23**, 327 (1977).

[23] H. J. C. Berendsen, J. P. M. Postma, W. F. van Gunsteren, A. DiNola and J. R. Haak, "Molecular dynamics with coupling to an external bath", *J. Chem. Phys.*, **81**, 3684 (1984).

[24] T. A. Andrea, W. C. Swope and H. C. Andersen, "The role of long ranged forces in determining the structure and properties of liquid water", *J. Chem. Phys.*, **79**, 4576 (1983).

[25] T. Amisaki, T. Fujiwara, A. Kusumi, H. Miyagawa and K. Kitamura, "Error Evaluations for the Design of Special-Purpose Processor for Molecular Dynamics Simulations", *J. Comp. Chem.*, **16**, 1120 (1995).

[26] S. Toyoda *et al.* (to be submitted).